

A. Krawczyk¹, A.G. Lyne², J.A. Gil¹ and B.C. Joshi^{2,3}¹ *Astronomical Centre, Pedagogical University, Lubuska 2, 65-265 Zielona Góra, Poland*² *University of Manchester, Nuffield Radio Astronomy Laboratories, Jodrell Bank, Macclesfield, Cheshire, SK11 9DL, UK*³ *National Center for Radio Astrophysics, Pune University Campus, P. O. Bag 3, Ganeshkhind, Pune, 411007, India*

2 May 2003

ABSTRACT

About 76 glitches in 25 pulsars have been reported to date. Most glitches are ‘giant’, with fractional increases of frequency $\Delta\nu_0/\nu_0 \sim 10^{-6}$. 25 glitches were analysed and presented by Shemar & Lyne (1996) who detected them mainly at Jodrell Bank during the monitoring of a sample of 279 pulsars in a regular timing programme up to MJD 49500. This paper is a continuation of their work up to MJD 50500. We present the detection and analysis of a further 14 glitches in 9 pulsars, 6 of which have glitched for the first time since monitoring had started. Eleven of these glitches are small ($\Delta\nu_0/\nu_0 \sim 10^{-9}$) and below the completeness threshold of Shemar and Lyne(1996). We report a giant glitch in PSR B1930+22, the second largest reported hitherto, with a $\Delta\nu_0/\nu_0 = 4.5 \times 10^{-6}$. We also report four recent glitches in PSR B1737–30 which continues to exhibit frequent glitches. Few of these pulsars show any recovery after the glitch.

1 INTRODUCTION

Two kinds of irregularities are observed in the rotation rates of pulsars, timing noise and glitches. Timing noise is a continuous wandering of the rotation rate, while glitches are characterized by a sudden increase in the rate, often followed by a period of relaxation. They are often revealed by the sudden onset of continually decreasing arrival time residuals. Glitches were first observed in the Crab and Vela pulsars (??) and it was soon realized that they can be important diagnostic tools for studying neutron star interiors (??). It is widely believed that these events are caused by sudden and irregular transfer of angular momentum from a faster rotating interior superfluid to the solid crust of the neutron star. The result is a sudden fractional increase in the rotational frequency ν_0 of the pulsar with a magnitude in the range $10^{-10} < \Delta\nu_0/\nu_0 < 5 \times 10^{-6}$. A characteristic feature of many glitches is a relaxation after the frequency jump, which may occur over a period of days, months or years. However, as we present in this paper, small glitches seem to show little significant relaxation after the glitch.

Although glitches are rather rare phenomena, an increasing number of these events have been reported recently (McKenna & Lyne 1990; Shemar & Lyne 1996; Wang et al. 2000; this paper), permitting more comprehensive statistical studies (Alpar & Baykal 1994; McKenna & Lyne 1990; Lyne, Shemar & Smith 2000). In this paper, we extend the analysis of the Jodrell Bank database by 2.5 year beyond that of Shemar & Lyne (1996) and seek to lower the detection threshold significantly.

2 OBSERVATIONS AND ANALYSIS

Observations were carried out at Jodrell Bank, mostly using the 76-m Lovell radio telescope, but also occasionally using the 30-m Mark II telescope. Measurements were made at intervals of between one and three months, while some, more interesting, pulsars were observed more often. The total list of pulsars that have been observed regularly in this programme at Jodrell Bank is presented in Shemar & Lyne (1996, their Table 1). Those authors analysed the data up to about MJD 49500. This work represents a more detailed study of the same data and also extends the analysis on their list of pulsars to about MJD 50500. The B1950 and J2000 names of these pulsars, their periods and characteristic ages, and the dates spanned by the observations are listed in Table 1. The main improvement in the analysis is a more careful calibration of the systematic effects which arose from the use of a variety of filterbanks and dedispersion procedures over the typically 16-year span of the observations. Greater care was also exercised in removing data which might have been affected by impulsive radio-frequency interference.

Both telescopes were equipped with dual-channel cryogenic receivers at observing frequencies centered close to 408, 610 or 1400 MHz. Each channel was sensitive to one hand of circular polarization. The data were dedispersed using filterbanks and folded synchronously with the nominal topocentric rotation period of the pulsar for sub-integration periods of between one and three minutes. An observation consisted typically of six such integrations which were stored on disk for subsequent processing.

Total intensity profiles were obtained by adding the six sub-integrations. These were then cross-correlated with a standard template to give pulse topocentric times of ar-

Table 1. Data span of Timing Observations used for analysis

PSR J	PSR B	Period (s)	Age (Kyr)	MJD RANGE	NO OF TOA
0157+6212	0154+61	2.35172383222	200	46866 – 50496	231
1740–3015	1737–30	0.60666591713	20	49243 – 51300	223
1801–0357	1758–03	0.92148958467	4400	46718 – 50586	124
1801–2304	1758–23	0.41579643949	60	49700 – 50687	71
1803–2137	1800–21	0.133634078897	16	49403 – 50600	127
1910–0309	1907–03	0.50460431337	3600	47392 – 50530	92
1919+0021	1917+00	1.27225573197	2600	48104 – 50640	175
1932+2220	1930+22	0.144455311469	40	49402 – 50583	112
2257+5909	2255+58	0.368245626351	1000	47523 – 50588	134

Table 2. Assumed Positions of 9 Glitching Pulsars

NAME	RA(J2000)	Dec(J2000)	Reference
B0154+61	01 57 49.91	+62 12 25.328	Martin (2001)
B1737–30	17 40 33.82(1)	–30 15 43.5(2)	Fomalont et al. (1997)
B1758–03	18 01 22.66	–03 57 55.39	Martin (2001)
B1758–23	18 01 19.803(9)	–23 04 44.2(2)	Frail et al. (1993)
B1800–21	18 03 51.401(4)	–21 37 07.34(7)	Fomalont et al. (1992)
B1907–03	19 10 29.686	–03 09 54.318	Martin (2001)
B1917+00	19 19 50.654	+00 21 39.848	Martin (2001)
B1930+22	19 32 22.693	+22 20 53.68	This paper
B2255+58	22 57 57.741	+59 09 14.917	Martin (2001)

rival which were then corrected to the Solar system barycentre using the JPL ephemeris DE200 (?). Assessment of arrival time residuals, which are the differences between actual pulse arrival times and times calculated from a simple rotational model, provides information about the behaviour of the pulsar rotation. The fitting procedure used a simple slow-down model involving rotational frequency and its first derivative. The analysis for each pulsar involves such a fit to a period of time which is devoid of any glitch activity. The timing residuals for the whole data set are then inspected visually for the presence of glitches. Pulsar positions assumed in this analysis are given in Table 2. Several of the positions were obtained from the same timing data described here, using data located well away from glitches (Martin 2001).

The parameters of each glitch were obtained from comparison of parameters before and after the glitch. Epochs of glitches were determined by requiring a continuity of phase across the glitch. Pre-glitch parameters were obtained by fitting a simple pre-glitch slow-down model of the form $\nu(t) = \nu_0 + \dot{\nu}_0 t$ to the data. The observed post-glitch frequency residuals are described as a function of the time t elapsed since the epoch of the glitch, relative to the pre-glitch ephemeris:

$$\Delta\nu(t) = \Delta\nu_p + \Delta\dot{\nu}_p t + \ddot{\nu}_p t^2/2 + \Delta\nu_1 e^{-t/\tau_1}, \quad (1)$$

where $\Delta\nu_p = \nu_p - \nu_0$ and $\Delta\dot{\nu}_p = \dot{\nu}_p - \dot{\nu}_0$ are differences between post-glitch and pre-glitch parameters. The last term in equation (1) describes an exponentially decaying transient component of post-glitch behaviour, while the penultimate term represents the large, approximately constant value of second derivative often seen following large glitches after any

short-term transient has decayed. Note that $\Delta\nu_p$ and $\Delta\dot{\nu}_p$ usually differ from the instantaneous changes in $\Delta\nu_o$ and its derivative because of the decaying components. Thus,

$$\Delta\nu_p = \Delta\nu_o - \Sigma\Delta\nu_1 \quad \text{and} \quad \Delta\dot{\nu}_p = \Delta\dot{\nu}_o + \Sigma\Delta\nu_1/\tau_1 \quad (2)$$

A more detailed description of the observation system and analysis can be found in the paper by Shemar & Lyne (1996).

3 RESULTS

The parameters of 14 new glitches found in 9 pulsars are given in Table 3, which shows the epoch of the glitch as a Modified Julian Date (MJD), pre-glitch frequency ν_0 and its first derivative $\dot{\nu}_0$ at that epoch, glitch fractional parameters, and the post-glitch frequency ν_p and its first derivative $\dot{\nu}_p$. The glitch epoch is estimated in the following manner. First, two solutions for the pulse phase across the glitch were obtained by extrapolating the pulse ephemeris before and after the glitch respectively. Then, the epoch was estimated from these phases by requiring that the pulse phase be continuous across the glitch. The errors quoted in brackets are twice the standard deviations obtained from the formal fits. However, this procedure could not be used for the glitch in PSR B1930+22 due to lack of sufficient number of measurements near the glitch as well as the large magnitude of the glitch. The relaxation parameters, $\dot{\nu}_p$, $\Delta\nu_1$ and τ_1 are usually insignificant in these glitches and are mentioned in the text where appropriate.

The frequency residuals for previously unpublished glitches are presented in the lower panels of Figs. 1, 3, 5–9

Table 3. Pre-glitch, glitch and post-glitch parameters for 14 glitches in 9 pulsars. Errors in the least significant place are given in parentheses.

PSR B	Epoch (MJD)	Pre-glitch Parameters		Glitch Parameters		Post-glitch Parameters	
		ν_0 (s^{-1})	$\dot{\nu}_0$ ($10^{-15}s^{-2}$)	$\Delta\nu_0/\nu_0$ (10^{-9})	$\Delta\dot{\nu}_0/\dot{\nu}_0$ (10^{-3})	ν_p (s^{-1})	$\dot{\nu}_p$ ($10^{-15}s^{-2}$)
0154+61	48504(1)	0.42521973638(2)	−34.1638(3)	2.46(6)	−0.04(1)	0.42521973743(1)	−34.1625(1)
1737−30	49451.7(4)	1.6483288501(3)	−1265.76(2)	9.5(5)	−0.32(2)	1.6483288657(7)	−1265.4(2)
	49543.93(8)	1.6483203659(8)	−1265.3(2)	3.0(6)	−0.68(2)	1.6483203709(6)	−1264.48(1)
	50574.5497(4)	1.6482078436(2)	−1264.02(1)	439.3(2)	1.261(2)	1.6482085677(2)	−1265.62(2)
	50941.6182(2)	1.6481684365(2)	−1265.56(1)	1443.0(3)	1.231(5)	1.6481708149(5)	−1267.12(6)
1758−03	48016(4)	1.0851988198(2)	−3.899(3)	2.9(2)	1.17(9)	1.08519882303(2)	−3.903(1)
1758−23	50055.0(4)	2.405065322(2)	−653.5(3)	22.6(9)	−0.08(2)	2.405065377(1)	−653.43(9)
	50363.414(4)	2.405047996(1)	−653.42(9)	80.6(6)	0.50(2)	2.4050481894(9)	−653.75(6)
1800−21	50269.4(1)	7.483583400(1)	−7496.36(8)	5.3(2)	0.195(4)	7.483583440(2)	−7497.8(3)
1907−03	48241(2)	1.9817509328(1)	−8.600(3)	0.60(6)	1.04(4)	1.98175093394(6)	−8.609(1)
	49219.85(2)	1.98175020655(9)	−8.606(2)	1.84(6)	0.28(3)	1.98175021019(6)	−8.609(1)
1917+00	50174(2)	0.78600232349(1)	−4.741(1)	1.29(3)	0.559(9)	0.78600232450(2)	−4.744(4)
1930+22	50264(20)	6.92210791(2)	−2756.4(1)	4457(6)	1.7(2)	6.92213877(2)	−2761.0(3)
2255+58	49463.2(2)	2.71557492794(4)	−42.436(1)	0.92(2)	−0.032(2)	2.71557493043(4)	−42.434(1)

and Fig. 11, and in the top panel of Fig. 10. They were obtained by performing local fits over about 50 days to the arrival time data, and presented relative to a simple slow-down model. Since most of the glitches presented in this paper are small, we also usually show their timing residuals in the upper panels of Figs. 1, 3, 5–9 and Fig. 11 for clarity of presentation. The number of available timing measurements between two glitches was small in the case of PSR B1737−30 making it difficult to obtain the frequency residuals in the manner described above except in case of two glitches. The timing residuals in all these pulsars show the familiar negative change in the gradient after the glitch, corresponding to a spin-up.

Below we describe detailed results of the search for glitches in the improved Jodrell Bank pulsar timing data base. Following Shemar & Lyne (1996), we give for each pulsar the conventional B-name, J-name (?) and the characteristic age $\tau = -\nu/2\dot{\nu}$.

3.1 PSR B0154+61 (J0157+6212, $\tau = 200$ kyr)

Although data on PSR B0154+61 have been collected at Jodrell Bank for more than 10 years since MJD 46866, this pulsar suffered its first observed glitch near MJD 48504. The glitch was quite small with the size of the frequency jump equal to 2.46×10^{-9} . The frequency and timing residuals are shown in lower and upper panels of Fig. 1, respectively. This glitch was not reported by Shemar & Lyne (1996), as it was below their completeness level of 5×10^{-9} in $\Delta\nu_0/\nu_0$.

3.2 PSR B1737−30 (J1740−3015, $\tau = 20.63$ kyr)

This pulsar exhibits frequent glitches and nine glitches have been reported in the past (McKenna & Lyne 1990; Shemar and Lyne 1996). Our analysis included observations carried out up to May 1999 for this pulsar (around 51300 MJD). We present four more glitches detected in these data. The timing residuals for the two smaller glitches are shown in Figure 2. The other two glitches were large with a $\Delta\nu_0/\nu_0$ exceeding 1.0×10^{-7} . The timing and frequency residuals for these glitches are shown in Figs. 3a and 3b and the glitch parameters for all the four glitches are presented in Table 3.

The cumulative fractional change in the rotation rate, $\Delta\nu_0/\nu_0$, for the pulsar is shown in Fig. 4. The dashed - dot line indicates the average rate of fractional spin-up due to glitches. The mean spin-up rate due to glitches, $\dot{\nu}_{glitch}$ (See Lyne et al. 2000), for this pulsar is about 1.4 percent of its spin-down rate. Thus, a fixed fraction 0.014 of the pulsar's slowdown is reversed by glitch activity and this is consistent with statistical estimate in other pulsars (Lyne et al. 2000). Shemar and Lyne (1996) noted that there are two types of glitches and this is evident from this figure. The larger glitches occur typically 800 days apart whereas the typical separation for all the glitches is of the order of 300 days.

3.3 PSR B1758−03 (J1801−0357, $\tau = 4,400$ kyr)

The rotational frequency and timing residuals for this pulsar are shown in Fig. 5. It suffered a glitch after 3 years of regular monitoring at Jodrell Bank and was not reported by Shemar & Lyne (1996), being below their sensitivity threshold. The size of the frequency jump is rather small, with

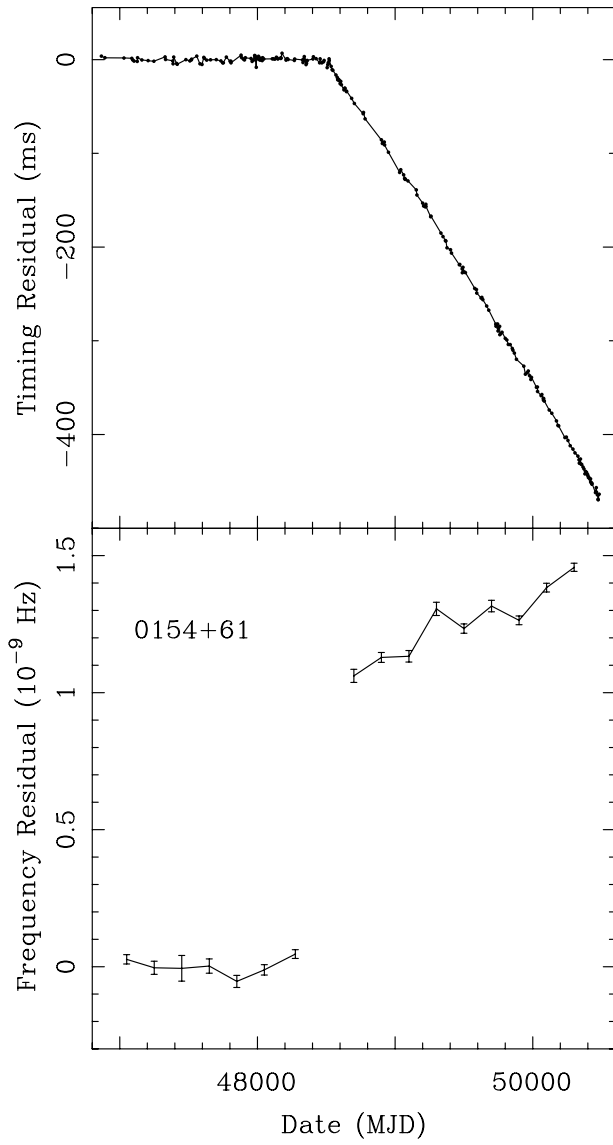


Figure 1. Rotational history of PSR B0154+61 with timing and frequency residuals presented in upper and lower panels, respectively. Errors are smaller than size of the points in the upper panel and are typically 0.6 ms

the fractional increase $\Delta\nu_0/\nu_0 \approx 3 \times 10^{-9}$. The only older pulsar which has been observed to glitch is PSR B1859+07 ($\tau = 4.5$ Myr). It is difficult to determine the exact date of the glitch because of the large gap of 140 days between observations. An estimate of the glitch epoch by assuming the continuity of pulse phase across the glitch indicates that the glitch occurred sometime near the beginning of 1990 (around MJD 48016). It was probably followed by a small relaxation, visible in the lower panel of Fig. 5.

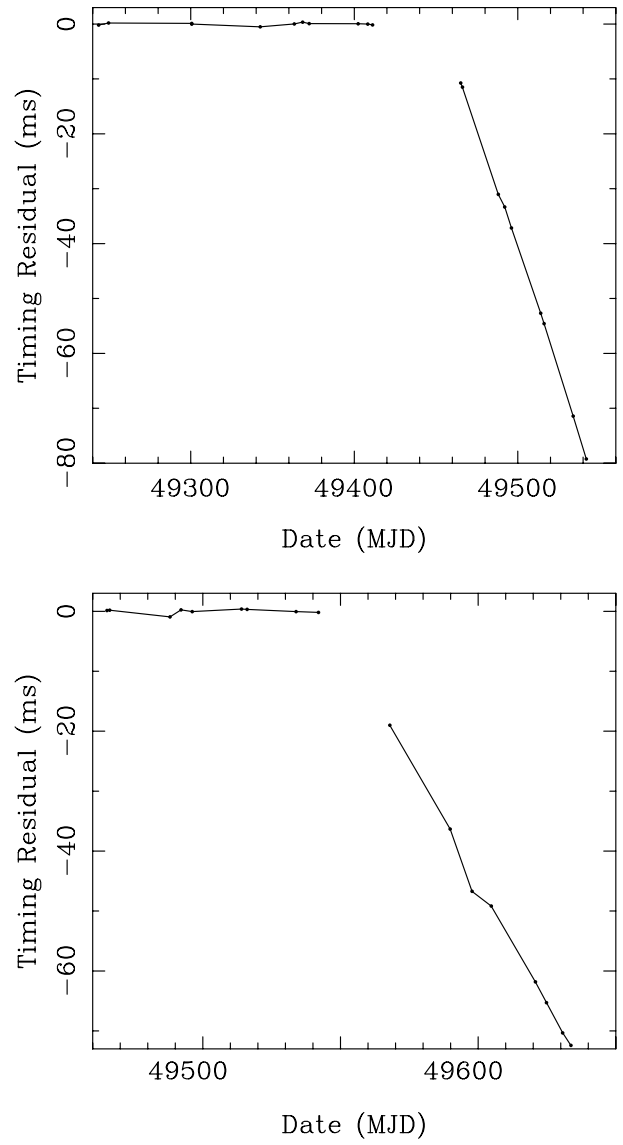


Figure 2. Timing residuals for the two small glitches in PSR B1737-30. The residuals for the glitch at MJD 49451 are presented in upper panel, while those for the glitch at MJD 49544 are shown in the lower panel, respectively. Errors are smaller than size of the points and are typically 0.2 ms

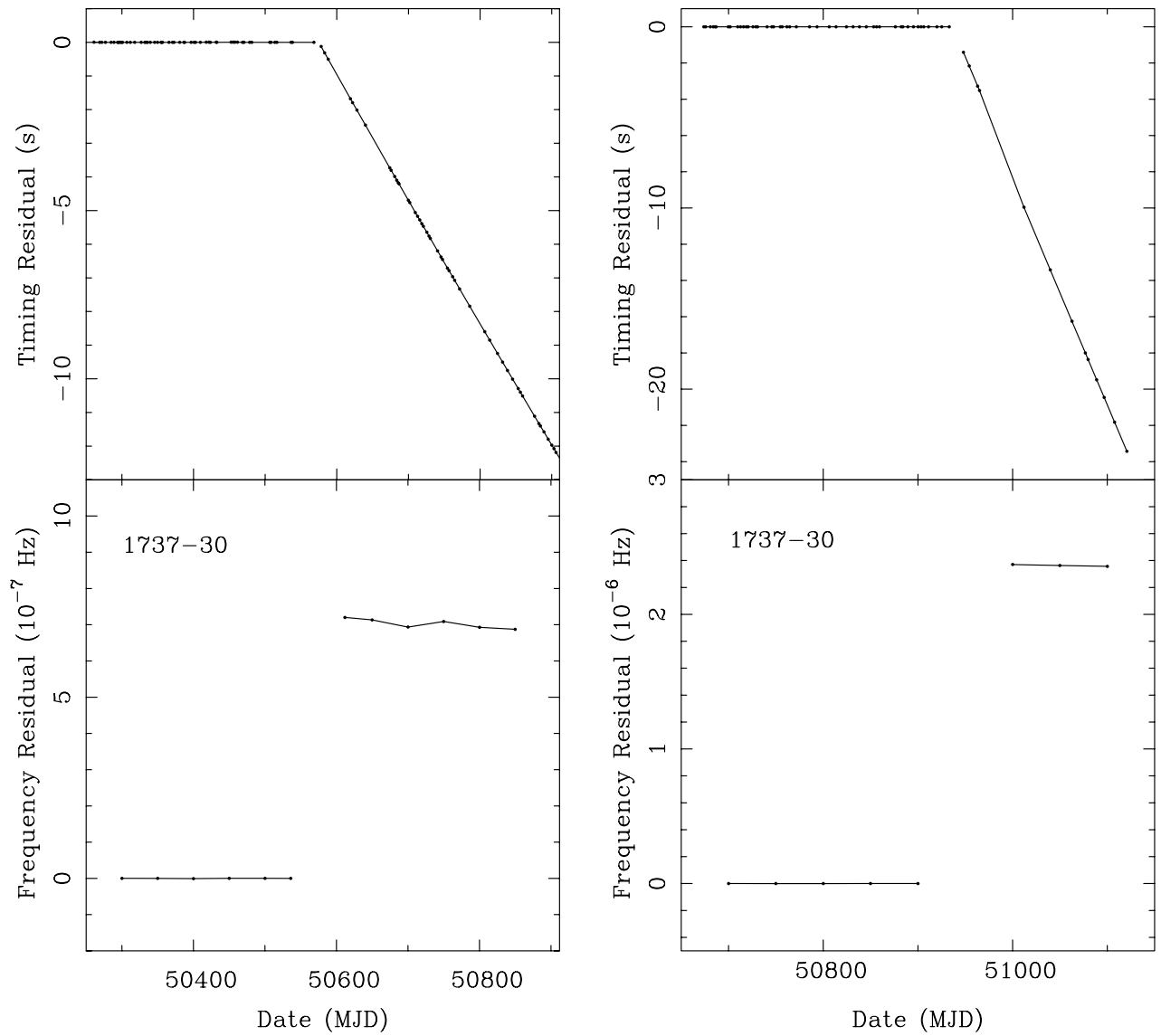


Figure 3. Rotational history of PSR B1737–30 with timing and frequency residuals presented in upper and lower panels, respectively. The glitch around MJD 50574 is shown in (a) and that around MJD 50941 in (b). Errors are smaller than size of the points in all plots and are typically 0.1 ms in the upper panel and of the order of 10^{-9} Hz in the lower panel

3.4 PSR B1758–23 (J1801–2306, $\tau = 60$ kyr)

The frequency and timing residuals for this pulsar are shown in Fig. 6. A total of 6 glitches have been detected in PSR B1758–23 since MJD 46697. The first three glitches were reported by Kaspi et al. (1993), the next one by Shemar and Lyne (1996) and we show two more recent glitches here. Four of these glitches were also reported by Wang et al. (2000). The first occurred around MJD 50055 and the second about a year later. Both newly-reported glitches are of moderate size, having magnitudes of $\Delta\nu_0/\nu_0 = 22.6 \times 10^{-9}$ and 80.6×10^{-9} , respectively. These values are consistent with those reported by Wang et al. (2000). The event reported in Shemar & Lyne (1996) is of similar size to the events presented here, while the glitches recorded by Kaspi

et al. (1993) are one order of magnitude larger, but still substantially less than those seen in Vela and other youthful pulsars. Thus all glitches in this pulsar are rather small. The post-glitch data analysis does not show any significant relaxation in this pulsar.

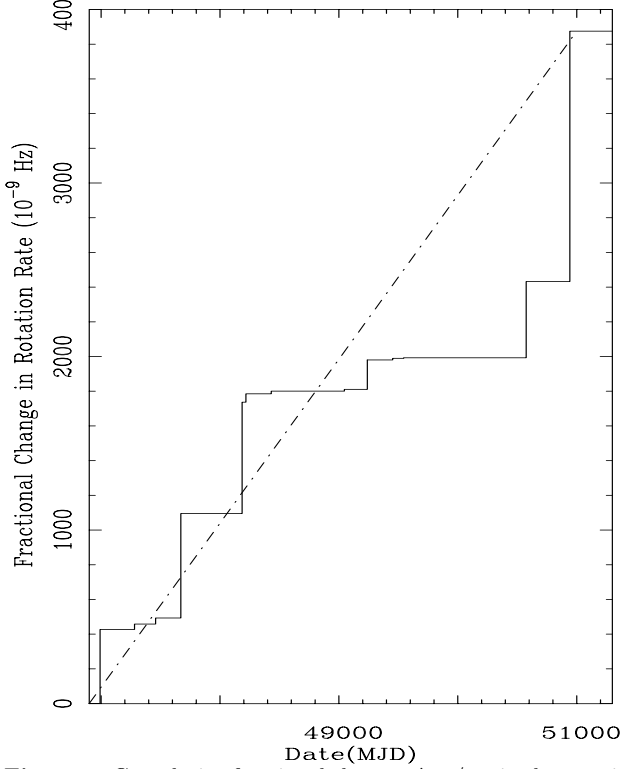


Figure 4. Cumulative fractional change, $\Delta\nu_0/\nu_0$, in the rotation rate of PSR B1737–30 for all the reported glitches. The average rate of fractional spin-up is indicated by the dashed line

3.5 PSR B1800–21 (J1803–2137, $\tau = 16$ kyr)

Shemar & Lyne (1996) reported a giant glitch with the third largest magnitude of all at the end of 1990, while we have found a small glitch with $\Delta\nu_0/\nu_0 = 5.3 \times 10^{-9}$ that occurred more than five years later around MJD 50269. The relatively dense data coverage around the event permitted the determination of the time of the event to within about one day. The timing and frequency residuals are presented in Fig. 7 (relative to data from about 1000 days between glitches). These plots show that the glitch was accompanied by a significant increase in the rate of slow-down.

3.6 PSR B1907–03 (J1910–0309, $\tau = 3,600$ kyr)

This is one of the oldest pulsars known to glitch and it suffered two rather small glitches. One of them occurred around MJD 48241 and the other about 1000 days later. In Fig. 8a and 8b, one can see the timing and frequency residuals for

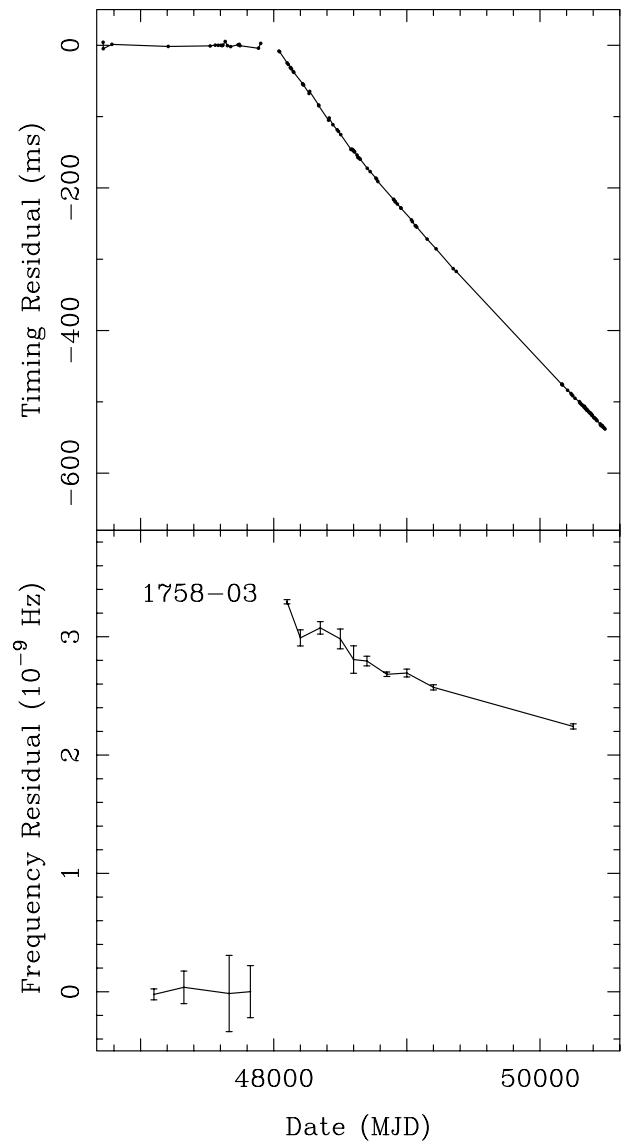


Figure 5. Rotational history of PSR B1758–03 with timing and frequency residuals presented in upper and lower panels, respectively. Errors are smaller than size of the points in the upper panel and are typically 0.4 ms

this pulsar corresponding to the two glitches. The fractional frequency increases are 0.6×10^{-9} and 1.84×10^{-9} , respectively. The first glitch is the smallest glitch known. Again, timing noise is probably the reason for irregular behaviour both before and after glitches. Both glitches reported here were below the threshold of the search of Shemar & Lyne (1996).

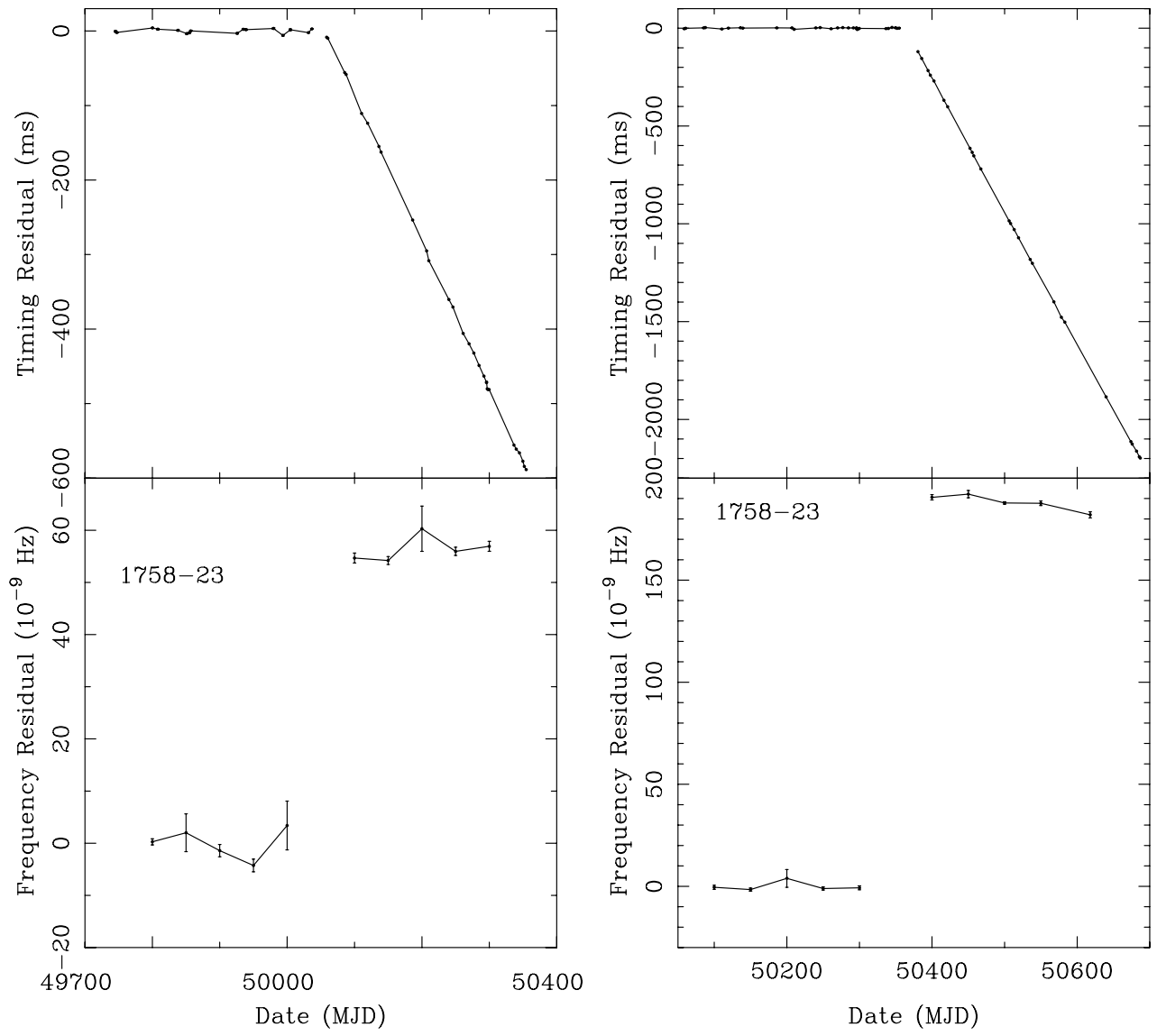


Figure 6. Rotational history of PSR B1758-23 with timing and frequency residuals presented in upper and lower panels, respectively. The glitch around MJD 50055 is shown in (a) and that around MJD 50363 in (b). Errors are smaller than size of the points in the upper panels and are typically 0.1 ms

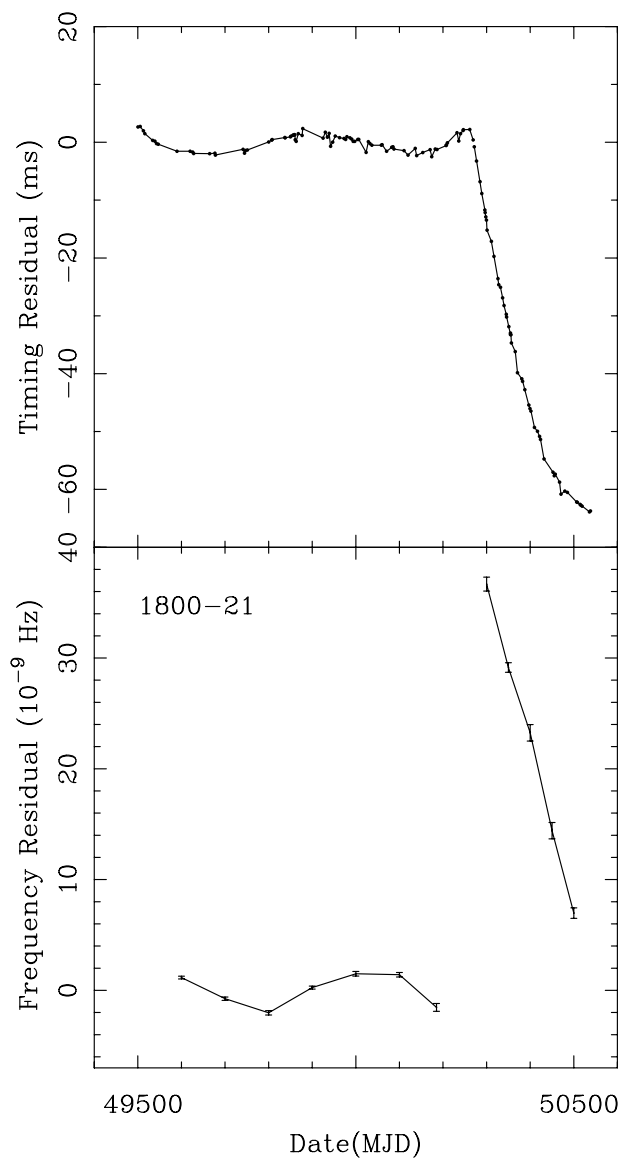


Figure 7. Rotational history of PSR B1800–21 with timing and frequency residuals presented in upper and lower panels, respectively. Errors are smaller than size of the points in the upper panel and are typically 0.2 ms

3.7 PSR B1917+00 (J1919+0021, $\tau = 2,600$ kyr)

Recently, around MJD 50174, the pulsar PSR B1917+00 suffered a small glitch, with fractional frequency increase $\Delta\nu_0/\nu_0 = 1.29 \times 10^{-9}$. There appears to be a small short-term relaxation after the glitch.

3.8 PSR B1930+22 (J1932+2220, $\tau = 40$ kyr)

A giant glitch occurred in this pulsar between MJD 50244 and 50284. The fractional frequency increase, $\Delta\nu_0/\nu_0 = 4457 \times 10^{-9}$, observed in this glitch is the second largest ever reported, marginally greater than the previous largest glitch in PSR B0355+54 (?; ?) and somewhat smaller than the recently reported glitch in PSR J1614–5047 (Wang et al. 2000). The frequency residuals and the frequency derivative for this glitch are shown in Figure 10. Removing the mean value of frequency from both pre-glitch and post-glitch data and expanding the frequency scale by a factor of 100 (Fig. 10b) reveals an almost linear relaxation of the rotation rate following a short term quasi-exponential relaxation. The exponential recovery can also be seen in the frequency derivative.

3.9 PSR B2255+58 (J2257+5909, $\tau = 1,000$ kyr)

PSR B2255+58 exhibited a small glitch at MJD 49463. Timing and frequency residuals corresponding to this glitch are presented in Fig. 11. This glitch is one of the smallest known with $\Delta\nu_0/\nu_0 = 0.92 \times 10^{-9}$.

4 DISCUSSION

Shemar & Lyne (1996) found 25 glitches in 10 pulsars after analysing about 2500 years of pulsar rotation in Jodrell Bank pulsar timing data base. Continuing this work we have found another 14 glitches in 9 pulsars in a further 1000 years of pulsar rotation in the improved and larger data base covering over about 7 years up to April 1997 (that is around 50500 MJD). We found 6 pulsars glitching for the first time, which increases the number of known glitching pulsars to 31. We also report new glitches in PSRs B1737–30, B1758–23 and B1800–21, which were already known as glitching pulsars. We report the smallest glitch ever observed, in PSR B1907–03 with $\Delta\nu_0/\nu_0 = 0.6 \times 10^{-9}$, and the second largest glitch, in PSR B1930+22 with $\Delta\nu_0/\nu_0 = 4457 \times 10^{-9}$. The fractional frequency increase in most of the glitches described in this paper is of the order of 10^{-9} . Thus, we detected 4 glitches which were not reported by Shemar & Lyne (1996) as they were below their threshold of 5×10^{-9} in $\Delta\nu_0/\nu_0$. We also found 10 more glitches in the epoch interval not covered by them. For those glitches newly found in the Shemar & Lyne interval, the average, the maximum and the minimum values of $\Delta\nu_0/\nu_0$ were 1.9, 2.9 and 0.6, while for those detected since then, the values were 646.2, 4457 and 0.92, respectively (all in units of 10^{-9}). This can be compared with corresponding values of the Shemar & Lyne (1996) search: 1072, 4368 and 1.2, respectively. They detected several giant glitches while our survey resulted mostly in the detection of rather small glitches.

The detection threshold of the present search for

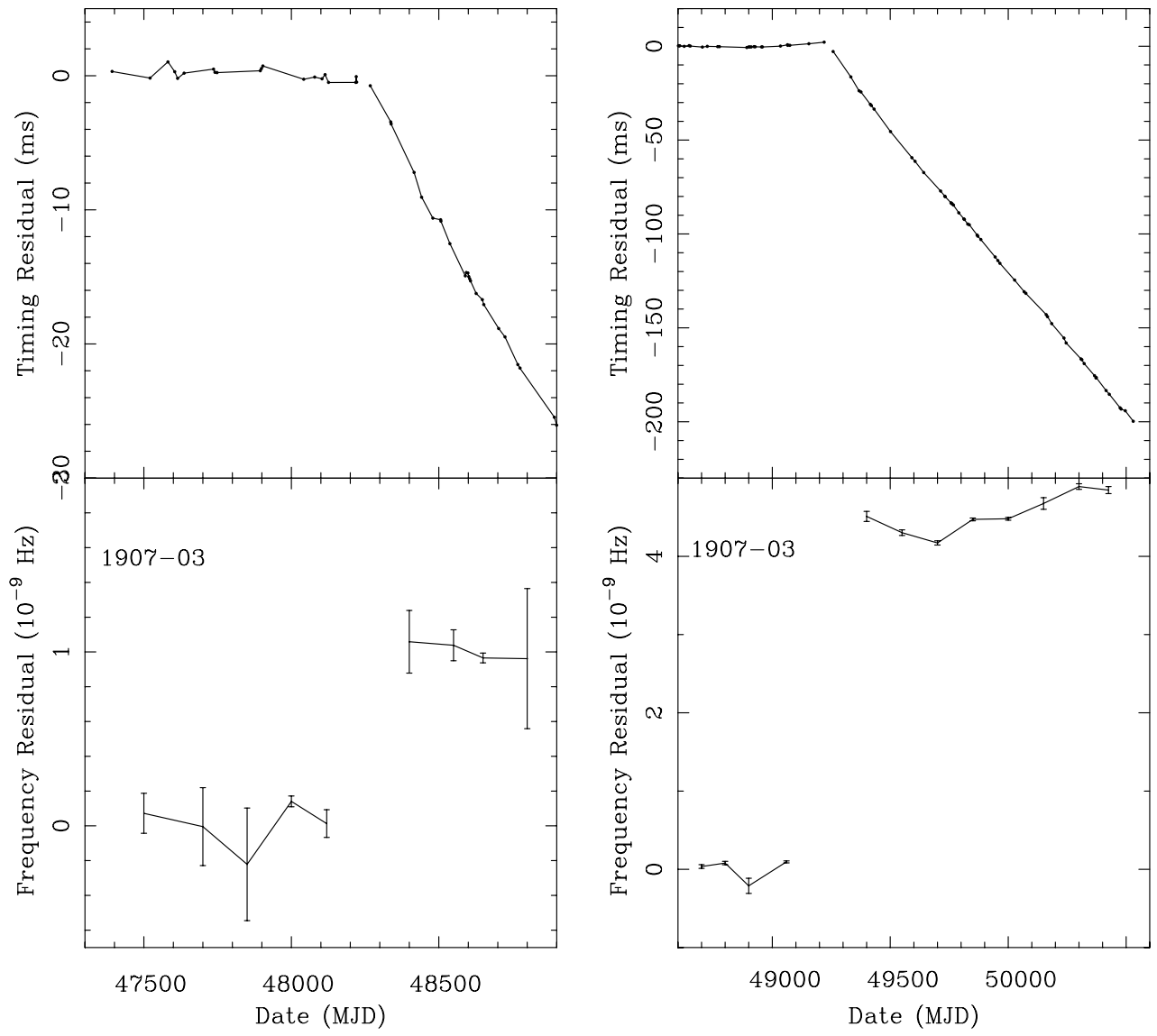


Figure 8. Rotational history of PSR B1907-03 with timing and frequency residuals presented in upper and lower panels, respectively for the glitch around MJD 48241 (a) and that around MJD 49219 (b). Errors are smaller than size of the points in the upper panel and are typically 0.3 ms and 0.2 ms respectively

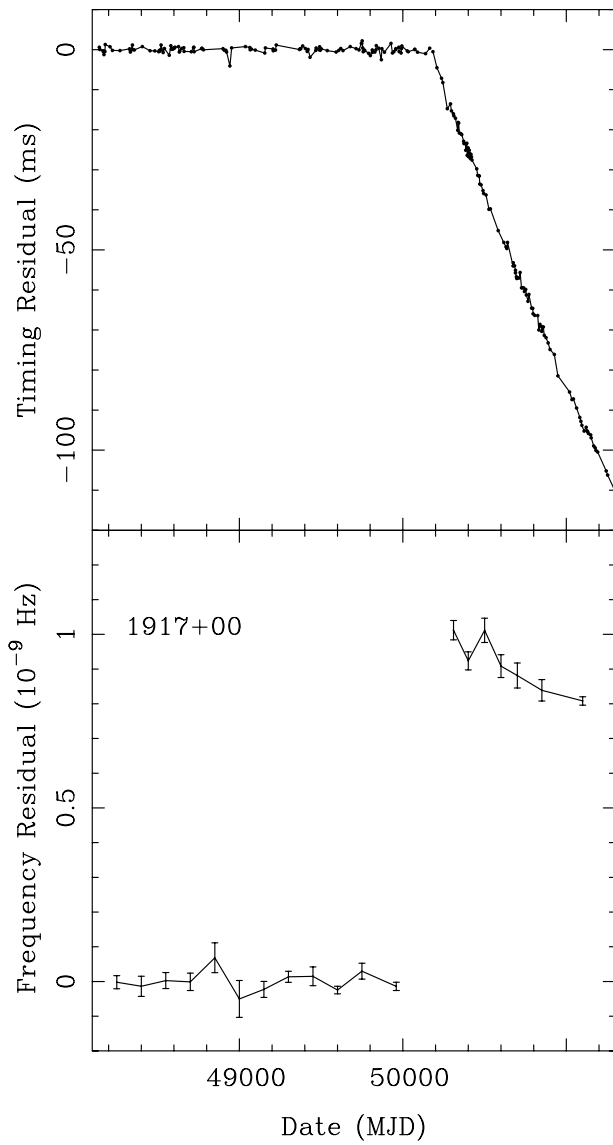


Figure 9. Rotational history of PSR B1917+00 with timing and frequency residuals presented in upper and lower panels, respectively. Errors are smaller than size of the points in the upper panel and are typically 0.6 ms

glitches varies significantly from one pulsar to another, depending upon the accuracy of the times-of-arrival, the density of the observations and the presence of timing noise intrinsic to the pulsar. We have conducted a number of simulations on a few dozen representative pulsars which had not glitched in our data set. The effects of a number of glitches of different magnitude in turn were introduced into the arrival time data of a pulsar. These data were then inspected using the glitch detection procedure described in section 2. As a result of these tests, we estimate that at least 90% of glitches with magnitude 2×10^{-9} have been detected. This is a factor of about 2.5 smaller than the threshold of Shemar & Lyne (1996). The detection of several glitches below the threshold of those authors indicates that the frequency

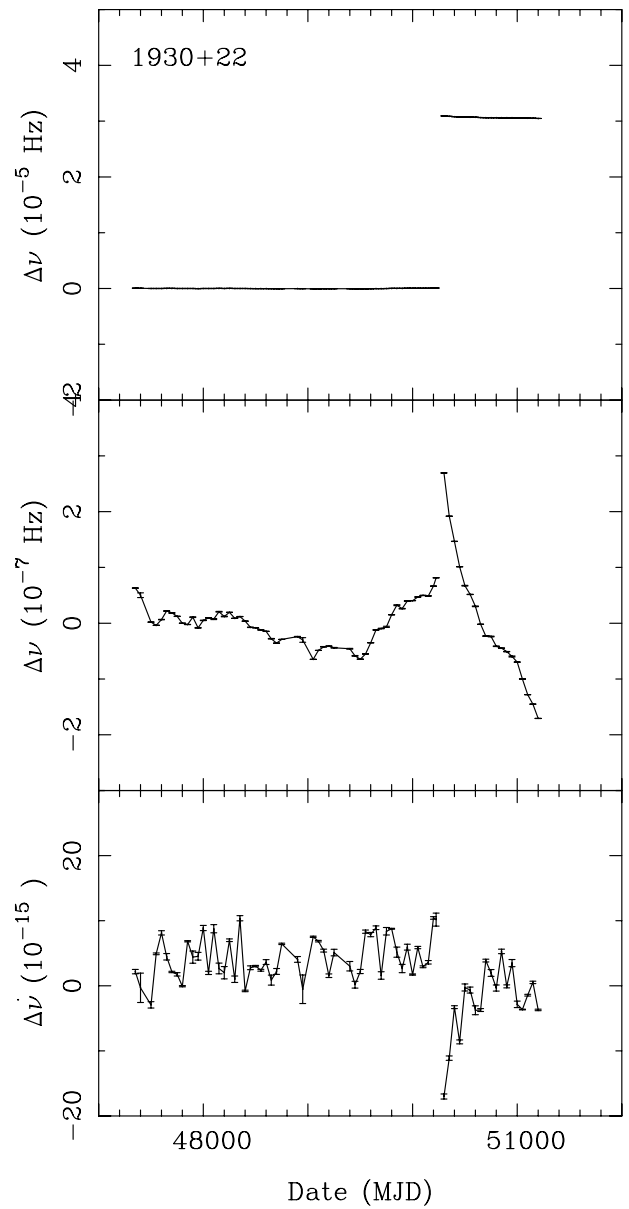


Figure 10. The rotational history of PSR B1930+22. a) The frequency residuals $\Delta\nu$ relative to a simple slow-down model involving the frequency and a constant value of its first derivative. b) As for (a) but with the mean frequency in each interval subtracted and the vertical scale expanded by a factor of 100. c) The frequency first derivative with a constant value of -2760.0 subtracted.

of occurrence of small glitches does not decrease for smaller sizes of glitch (e.g. Lyne *et al.* 2000).

We confirm the observation of Shemar & Lyne (1996) and Lyne *et al.* (2000) that the dominant effect of glitches, particularly the smaller ones, is a sudden increase in rotational frequency with very little or no recovery. The age range of the glitching pulsars is broad, from 16 thousand to 4.4 million years, including PSR B1758-03, which is now the second oldest glitching pulsar.

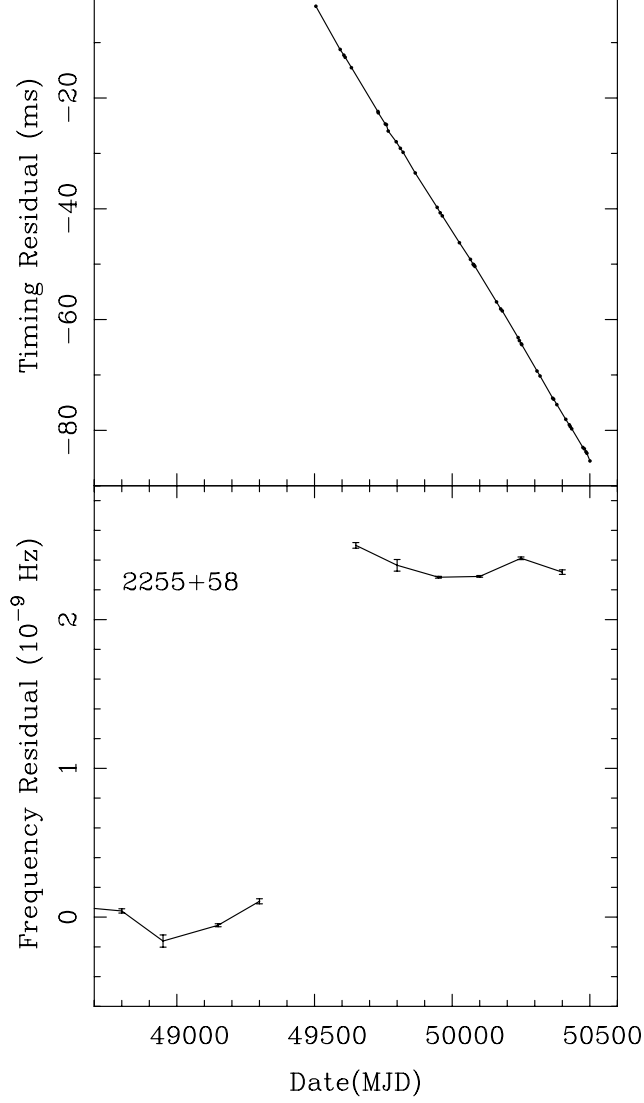


Figure 11. Rotational history of PSR B2255+58 with timing and frequency residuals presented in upper and lower panels, respectively for the glitch around MJD 49463. Errors are smaller than size of the points in the upper panel and are typically 0.04 ms

Acknowledgements This work is supported in part by the KBN Grant 2 P03D 015 12 of the Polish State Committee for Scientific Research.